

3D printing and photonics

Kevin Cook and John Canning

interdisciplinary Photonics Laboratories, School of Electrical & Data Engineering, University of Technology Sydney (UTS), NSW 2007 & School of Chemistry, The University of Sydney, NSW 2006, AUSTRALIA

**Corresponding author: kevin.cook@uts.edu.au*

Abstract: Recent progress in the field of 3D-printed photonic devices and their tremendous potential in sensing applications is reviewed. This truly disruptive technology has led to the realization of polymer optical fibres made from 3D-printed preforms, planar rib waveguides, lens arrays and prisms, all precursors for coming 3D printing of silica and other components.

1. Introduction

The popularity of 3D printing, or additive manufacturing, has grown at a relentless pace. High calibre printers are becoming indispensable tools in labs and workshops the world over. The benefits reach across areas from rapid prototyping to the development of medical devices and the creation of art [1]. By far the most common printing technique is fused deposition modelling (FDM), around since the 1980s [2] and the working principle behind today's cheapest polymer printers. A polymer filament, such as acrylonitrile butadiene styrene (ABS) or polylactic acid (PLA), is continuously fed through a hot nozzle to create a controlled ooze which is deposited on a heated platform. Control of this deposition is achieved by translating the nozzle in the x - y horizontal plane to outline a "slice" of an object to be printed. The bed is lowered, or the nozzle raised, in the z direction in increments between each layer to build a 3D object. Competing with FDM is SLA 3D printing, essentially stereolithographic using a UV or visible light source, often a lamp or LED. In this process photopolymerisation of a monomer solution is employed. It has the advantage of using 2D projection to accelerate 3D printing whilst remaining relatively low cost. However, the range of suitable materials can be lower although significant material development is changing this. This approach is often used for dental and medical applications where high resolution, typically in the tens of microns domain but in principle limited by the optical wavelength used to cure the polymer is required. Other techniques include Selective Laser Sintering (SLS) which extends the range of printable materials to glass, ceramics and even metal. Here, a (e.g. CO₂) laser is scanned over a layer of powdered material to fuse together particles. After each scan the powder bed is lowered and fresh material spread over the previous layer and then fused – a 3D object is formed [3].

The ramifications for photonics of this disruptive technology are starting to be felt, with 3D printing of transparent optical components becoming a reality. Early work reported direct printing of short sections of polymer optical fibre [4] and "light pipes" [5], in one case used as an effective channel to guide light in an optical fibre endoscope smartphone configuration (the package itself 3D printed) [6]. In other work, 3D printing of optical phantoms – objects used for the testing and evaluation of medical imaging devices – have been demonstrated using transparent plastic [7,8]. Printing of plastic micro lenses and customized ophthalmic lenses are now commercially available [9]. 3D printing offers advantages over its subtractive manufacturing counterpart, removing any grinding/polishing and providing the freedom to print arbitrary shapes.

Polymer offers many advantages to optical sensing. For example, fibre Bragg gratings (FBGs) in polymer fibre have remarkable wavelength tunability for increased sensing dynamic range [10]. However, silica glass is still the popular choice for sensing because of its chemical resistance and high temperature performance [11]. But there has been little work on 3D glass printing. Early work adopted an FDM approach using soda lime glass [12]; the printed structures were limited to single-wall (vase-like) structures with a resolution of several millimeters. Other work used selective laser melting (SLM) with a CO₂ laser to print structures with soda lime glass [13] – again, the resolution was coarse and surface roughness high. In 2017, printing high-purity silica was demonstrated using SLA with a UV-curable monomer doped with silica nanoparticles. The printed part was initially opaque but after thermal debinding of the monomer and high-temperature sintering in an oven to vaporise the organic component, a highly-transparent silica object is achieved with spatial features of 10s of μm [14]. Whilst shrinkage issues and losses need addressing, this work is a milestone in 3D printing.

Here a brief review is presented showing how 3D printing can benefit photonics, across optical fibre fabrication, planar waveguides, lenses and prisms.

1.1 Optical fibre from 3D printed preforms

To investigate the printing of optical fibre preforms, a deltasine-style printer [15] was employed with “modified ABS” (a propriety polystyrene mixture containing styrene-butadiene-copolymer and polystyrene which we labelled “SBP”). A simple air-structured preform design with an outer diameter of $\phi = 1.6$ cm and 6 air channels surrounding a central core was designed. Each channel had a diameter $\phi_{\text{hole}} = 0.2$ cm and were evenly spaced around the periphery (Fig.1(a)). The preform length was 10 cm and took 6 hours to print. Unlike conventional stacking of structured preforms the process is automated, demonstrating how industrial fabrication costs and time can be reduced. The final printed preform is shown in Fig.1(b). It was drawn into fibre using a polymer draw tower with an outer diameter $\phi_{OD1} \sim 712$ μm and $\phi_{OD2} \sim 605$ μm for the major and minor axes respectively, whilst the core diameter is $\phi_{c1} \sim 221$ μm and $\phi_{c2} \sim 148$ μm for the major and minor axes respectively (Fig.1(c)). Light is found to guide in all regions of the fibre but further improvements in fabrication, for example the use of hole pressurisation, will help reduce the thickness of strands between air holes leading to core confinement. Cut-back losses were found to be: $\alpha \sim 1.5$ dB/cm @ 632 nm, $\alpha \sim 0.75$ dB/cm @ 1064 nm, and $\alpha \sim 1.51$ dB/cm @ 1550 nm, demonstrating complete removal of scatter from the 3D printed layers of the preform [16].

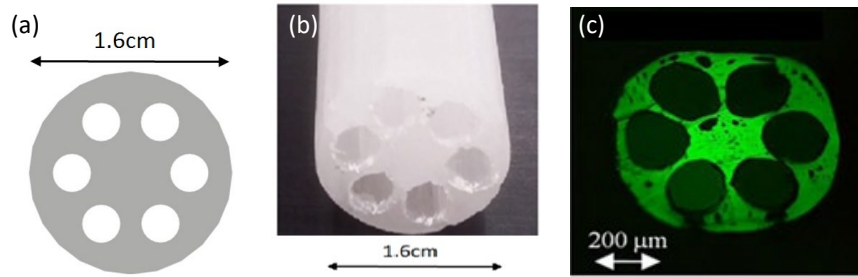


Figure 1(a): Cross-section of designed airstructured preform; (b): Photo of final printed preform; (c): Visible guidance of 515 nm light.

A step index fibre was also printed. The selected filaments are both off-the-shelf products and are summarised in Fig.2(a). SBP ($n_{\text{SBP}} = 1.456$) made up the preform cladding and modified PETG ($n_{\text{MPETG}} = 1.527$) made up the core ($\phi_{\text{core}} = 8.0$ mm; cladding $\phi_{\text{clad}} = 18.6$ mm). The preform was printed using a dual extruder printer (Flashforge Dreamer) with the same resolution as the deltasine printer. Fig. 2(b) shows the printed preform, showing step-index guidance when light from a laser pointer ($\lambda = 532$ nm) is coupled into one end.

(a)	Core filament	Cladding filament
Material	"Modified polyethylene terephthalate glycol" (MPETG)	"Polystyrene mixture containing styrene-butadiene-copolymer and polystyrene" (SBP)
Appearance	Clear/transparent	Clear/transparent
Source	Commercially-available	Commercially-available
Refractive index	1.527	1.456
Printing temperature (°C)	225	230

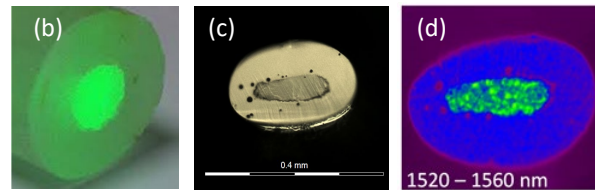


Figure 2(a): Table summarising the filaments used for core and cladding; (b) Photo of final printed preform showing step-index guidance; (c) Microscope image of the cross-section of final printed fibre; (d) Image of core-guided NIR light.

The preform was drawn to fibre under similar conditions to those used for the air-structured fibre (details in [17]). The cross-section of the drawn fibre is shown in Fig. 2(c), exhibiting an elliptical shape that most likely arises due to the relaxation of stresses created during the layer-by-layer printing process (the preform was printed with its long edge on the printer bed). The outer diameters of the fiber major and minor axes are $\phi_{OD1} \sim 283$ μm and $\phi_{OD2} \sim 204$ μm , while the core diameters are $\phi_{c1} \sim 171$ μm and $\phi_{c2} \sim 60$ μm , respectively. The fibre is expected to be highly multimode with a V-number $V > 60$. It guides light in the core in both the visible and NIR. Fig. 2(d) shows core confinement of NIR light from an Erbium-doped fibre amplifier (EDFA). Cut-back measurements indicate lower losses than the air-structured fibre ($\alpha \sim 0.64$ dB/cm @ 543 nm, $\alpha \sim 0.44$ dB/cm @ 1047-1052 nm; $\alpha \sim 0.94$ dB/cm @ 1550 nm [17]).

3D-printed rib waveguides

Using the same MPETG polymer filament as the previous section, a Flashforge Creator Pro printer (similar resolution as the Dreamer) was used to print rib waveguides on a planar substrate with rectangular dimensions (length $l = 50$ mm, width $w = 15$ mm, height $h = 1.5$ mm). The rib waveguides were fabricated with a single pass of the printer nozzle, forming lines of width $434 \mu\text{m}$ and height $181 \mu\text{m}$ (Fig. 3(a)). Fig. 3(b) shows the output mode profile generated using the ASE output of an EDFA ($\lambda \sim 1520$ to 1560 nm) butt coupled by fibre to the input of the waveguide. Coupled HeNe laser light (632 nm) and an ytterbium doped fibre amplifier (YDFA, $\lambda \sim 1000$ to 1100 nm) had losses ranging from $\alpha \sim (11.86 - 15.03)$ dB/cm. Fig.3(c) shows a 50:50 optical coupler with a 4 mm interaction length; the output is shown in Fig.3(d) with mode images in Fig.3(e) and Fig.3(f).

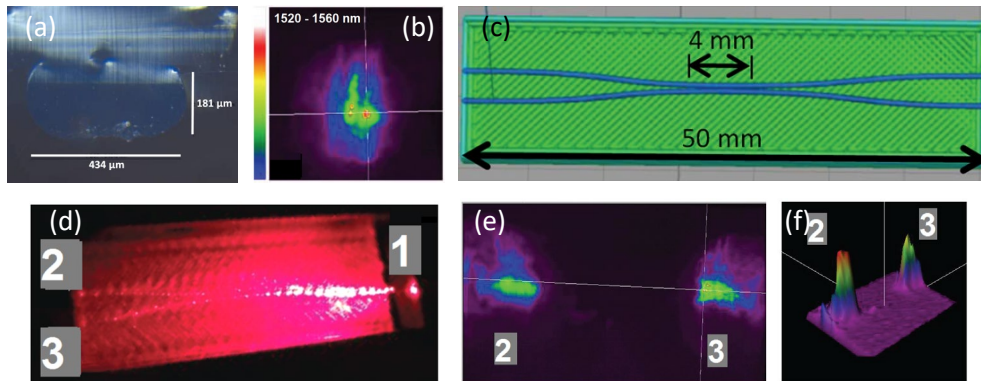


Figure 3(a): Optical microscope image of the polished end-face of one waveguide; (b) Mode image of NIR guidance; (c) Design of 50:50 optical coupler; (d) Top view of coupler indicating splitting; (e-f) Leaky modes exiting ports 1 & 2.

1.2 Other work

Initial prototypes for 3D-printed lenses and prisms are shown in Fig 4(a) & (b). Cheap, disposable 3D printed prisms are ideal for field deployable surface plasmon resonance (SPR) work where the plane surface is coated with gold. In other work, we routinely print customised packages for photonic devices such as rail strain/temperature sensors (Fig.4(c)) and handheld, smartphone-driven spectrometers (Fig.4(d)) [18].

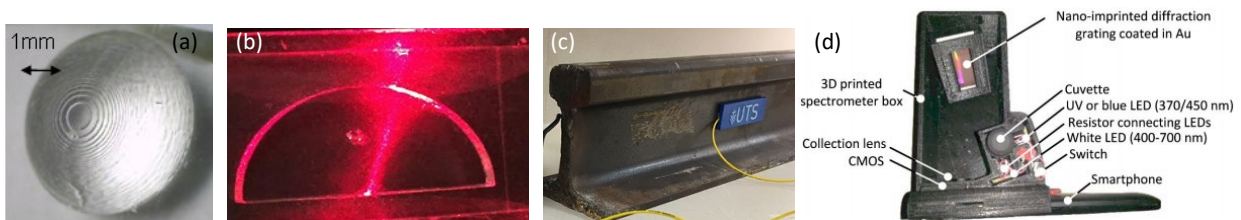


Figure 4: 3D-printed (a) lenses; (b) prisms; (c) fibre sensor packaging; and (d) portable spectrometers.

2. Conclusion

A range of photonic technologies are now amenable to increasingly low cost 3D printing, marking a radical onset in optical manufacture. Arbitrary designs almost impossible by other means are within reach. With silica printing now on the horizon, a paradigm shifting in manufacturing technology is coming to fruition.

3. References

- [1] H. Lipson and M. Kurman, John Wiley & Sons, (2013).
- [2] S.S. Crump, US Patent 5121329 A, (1992).
- [3] E.D. Dickens *et al.* US Patent 5990268 A, (1999).
- [4] T. Pereira *et al.* ACM Transactions on Graphics (TOG) TOG Homepage archive, 33, 3, Article No. 24, (2014).
- [5] K. Willis *et al.* UIST '12 Proc. 25th Ann. ACM Symp. User Interface Software & T, PP 589-598, (2012).
- [6] M. A. Hossain *et al.* Opt. Lett., **41** (10) 2237, (2016).
- [7] J. Wang *et al.* Opt. Lett. 39, 3010 (2014).

- [8] P. Diep *et al.* Biomedical Optics Express. 6 (11), 4212 (2015).
- [9] www.luxexcel.com
- [10] Z. Xiong *et al.* IEEE Photonics Technology Letters, 11 (3), 352 (1999).
- [11] S. Bandyopadhyay *et al.* Opt. Lett. 33, 1917, (2008).
- [12] J. Klein *et al.* 3D Printing and Additive Manufacturing, 2 (3), 92 (2015).
- [13] J. Luo *et al.* ASME. J. Manuf. Sci. Eng. (2014).
- [14] F. Kotz *et al.* Nature, 544, 337 (2017).
- [15] C. Bell, Technology in Action, Apress, (2015).
- [16] K. Cook *et al.* Opt. Lett. 40 (17), 3966 (2015).
- [17] K. Cook *et al.* Opt. Lett. 41, 4554 (2016).
- [18] M.A. Hossain *et al.* Opt. Lett. 40, 1737 (2015).